Journal of Environmental Management 213 (2018) 382–391

Contents lists available at ScienceDirect

Journal of Environmental Management

journal homepage: www.elsevier.com/locate/jenvman

Research article

Hydrological controls on nitrogen (ammonium versus nitrate) fluxes from river to coast in a subtropical region: Observation and modeling

Xinjuan Gao [a], Nengwang Chen [a, b, *, *], Dan Yu [a], Yinqi Wu [a], Bangqin Huang [a, b]

[a] Fujian Provincial Key Laboratory for Coastal Ecology and Environmental Studies, College of the Environment and Ecology, Xiamen University, Xiamen, China
[b] Key Laboratory of the Coastal and Wetland Ecosystems, Xiamen University, Xiamen, China

ARTICLE INFO

Article history:
Received 14 November 2017
Received in revised form
11 February 2018
Accepted 14 February 2018

Keywords:
Nutrient
LOADEST model
Flood
Storm
Eutrophication
Climate change

ABSTRACT

Increased anthropogenic nutrient input and losses has caused eutrophication problems in freshwater and coastal ecosystems worldwide. High-frequency observations and modeling of river fluxes in subtropical regions are required to understand nutrient cycling and predict water quality and ecological responses. In 2014, a normal hydrologic year, we carried out daily sampling of the North Jiulong River in southeast China, which drains an agricultural watershed and experiences the Asian monsoon climate. We focused on the distinct characteristics of two important inorganic nitrogen forms (ammonium and nitrate). Our results show contrasting hydrological controls on the seasonal timing and magnitude of ammonium and nitrate concentrations and loads, likely due to differing sources and transport pathways (surface runoff versus baseflow) to the river. Both nitrogen concentrations were enriched in the dry season and diluted in the wet season. Arrival of rains in the pre-wet period in March caused a "first flush" peak event with the highest concentrations of the year, during which ammonium peaked two weeks earlier than nitrate. In contrast, the majority of nitrogen transport occurred during the lower concentrations of the wet season, with seven storms inducing flood events that lasted 24% of the time, contributed 52% of the runoff, and exported 47% of the ammonium and 42% of the nitrate. We found that seasonally piecewise LOADEST models (for pre-wet, wet and post-wet periods) performed better (5–8% error) than a year-round model (12–24% error) in estimating monthly nitrogen loads. However, not all nitrogen dynamics are easily synthesized by this approach, and extreme floods might produce a greater deviation in estimating nitrogen loads. These findings represent important implications for coastal ecology and provide opportunity on improving observation and modeling.

1. Introduction

Human activities and climate change have caused estuaries and coastal ecosystems worldwide to receive increased riverine nutrient loads (Howarth, 2008; Paerl, 2006; Peñuelas et al., 2013; Strokal et al., 2016; Turner and Rabalais, 1994). Increasing nitrogen (N), principally in the form of inorganic N (nitrate, nitrite, and ammonium) has led to a series of ecological and environmental problems (e.g. water quality deterioration, eutrophication, and harmful algal blooms) that present large threats to socio-economic development and human health (Billen and Garnier, 2007; Davidson et al., 2014; Paerl et al., 2011; Reed et al., 2016). Many studies have demonstrated that wet season and accompanied storm events contribute to the majority of annual nutrient loading to river and coastal water (Adame et al., 2016; De Carlo et al., 2007; Zhang et al., 2009). Aquatic ecosystems are sensitive to the changing nutrient loading and their elemental ratios over seasons and storm events (Chen et al., 2015; Cornelis et al., 2011; Corriveau et al., 2013; Sigleo and Frick, 2007). River N loading to the coastal waters of China have been predicted to increase continually through 2050 (Strokal et al., 2014). Anthropogenic factors (agriculture development, sewage discharge, dam construction, and land use change) within watersheds and climate factors (watershed precipitation and discharge) synergistically affect the magnitude and timing of nutrient loading (Johnson et al., 2007; Statham, 2012). Coastal areas in China are affected by the Asian monsoon climate which is characterized by strong seasonal variations in

* Corresponding author. College of the Environment and Ecology, Xiamen University, Xiamen 361102, PR China.
E-mail address: nwchen@xmu.edu.cn (N. Chen).

https://doi.org/10.1016/j.jenvman.2018.02.051
0301-4797/

precipitation and frequent storm events. Therefore, observation and modeling of river nutrient fluxes at the seasonal scale has become an important basis for managing watershed nutrients and mitigating coastal eutrophication.

Several models have been developed to simulate river N load. For instance, SWAT (Soil and Water Assessment Tool) estimates nutrient yields in surface runoff and identifies critical source areas in watershed and large river basins (Arnold et al., 1998). WASP (Water Quality Analysis Simulation Program) has been used to estimate the influence of nutrient loads on the water quality of Tampa Bay, U.S.A (Wang et al., 1999). HSPF (Hydrological Simulation Program-Fortran) quantifies N exported annually from the catchment of the Great Barrier Reef, Australia (Hunter and Walton, 2008). These models require detailed, high quality input data which are often difficult to obtain in large catchments. The Load Estimator (LOADEST), a statistical model developed by USGS, makes use of limited flow and water quality datasets to set up a regression formula of corresponding pollutant fluxes, and then estimates their loads at different time scales (Runkel et al., 2004). The LOADEST model is considered to be a useful management tool and has been widely applied to river N load estimations. Johnson et al. (2007) explored nitrate fluxes of Fall Creek watershed in central New York during 1972–2005. Mast, (2013) used LOADEST to analyze temporal trends in stream N over two periods (1970–2010 and 1990–2010). Pellerin et al. (2014) explored the ability of high frequency measurements of nitrate concentration to improve the accuracy of monthly nitrate loads. The LOADEST model has also been optimized by adjusting sampling frequency and obtaining storm samples (Duan et al., 2014; Park and Engel, 2014; Park and Engel, 2015; Toor et al., 2008). In contrast to this abundance of previous work to estimate nitrate loading, modeling efforts on river ammonium loads are scarce. Considering ammonium and nitrate separately, rather than just total dissolved inorganic N is important because they can have different sources, biogeochemical behaviors, and potential ecological effects (Domingues et al., 2011; Dugdale et al., 2007; Tamminen, 1995).

We carried out daily sampling in a hydrologic year (2014) to better understand the hydrological processes controlling seasonal and flood-event N fluxes from the main (North) branch of the Jiulong River, which drains an agricultural watershed. We focused on determining the contrasting characteristics and behaviors of two inorganic N forms (ammonium versus nitrate) under the extreme rainfall variations that occur in the Asian monsoon climate. We first present seasonal patterns of nitrate and ammonium concentrations and loads, and then use the LODEAST model approach to determine total fluxes from the river, including developing and evaluating a seasonally piecewise LOADEST model (for the pre-wet, wet, and post-wet periods). Finally, the hydrological controls on river N (ammonium versus nitrate) export are summarized, and perspectives on future observations and modeling of N loads are discussed.

2. Materials and methods

2.1. Description of study site

The Jiulong River watershed is located in southeast China, comprised of the North, West and South Rivers (Fig. 1). The North River is the main branch, with a drainage area of 9570 km^2. Its length to the mouth (Jiangdong) is around 274 km, traversing an elevation change of 325 m. The topography in the North Jiulong River (NJR) is mostly hilly (91% of the catchment area has an altitude greater than 200 m). Land use is comprised of 78% forest (mostly artificial), 16% arable land, 3% urban and residential land, 2% water, and 1% bare and grassland (based on information from the 2007 Landsat Thematic Mapper). Six major dam reservoirs have been constructed in the main branch of the river mainly for hydropower generation and flood control (Wang et al., 2010). The NJR flows through four cities/counties (Longyan, Zhangping, Hua'an and Changtai) and a part of Zhangzhou city, with approximately 1.5 million people in total. Longyan city is located furthest upstream, where animal farming has become the dominant industry since the 1990s. The other counties are downriver and comprised of predominantly agricultural and forest land. The Jiulong River and adjacent estuary have suffered nutrient (N and P) enrichment and eutrophication problems during the past three decades (Chen et al., 2013; Li et al., 2011; Yan et al., 2012).

2.2. Daily sampling and laboratory analysis

Daily surface water samples in 2014 were manually collected at the mouth of the NJR (at the Jiangdong auto monitoring station, operated by Xiamen Environmental Monitoring Center). About 50 mL of water was filtered immediately (0.45 μm membrane) after each sampling, and stored frozen at −20 °C at Jiangdong until monthly delivery to Xiamen University for analysis. The thawed water samples were analyzed by segmented flow automated colorimetry using the manufacturer's standard procedures (San++ analyser, The Netherlands) for ammonium (NH_4–N) and the sum of nitrate and minor nitrite (called NO_3–N here). Dissolved inorganic nitrogen (DIN) was summed from NO_3–N + NO_2–N + NH_4–N. Sampling, preservation and transportation of the water samples to the laboratory were conducted by standard methods for surface waters (American Public Health Association, 2005). The precision for the DIN components was estimated by repeated determinations of 10% of the samples and the relative error was 3–5%. Commercial standard reference materials were used to check the instrument performance.

2.3. Auxiliary data collection and data analysis

Hourly rainfall records from four weather stations within the catchment were obtained from Weather China (http://www.weather.com.cn/). Daily river discharge was obtained from a nearby hydrological station (Punan) and was extrapolated to the sampling site (Jiangdong) using the ratio (1.08) of the catchment area between them (Fig. 1). Baseflow was estimated using an automatic segmentation procedure (BFI (F): Smoothed Minima method). The designation of a flood event was applied only to flow increases that exceeded 2 times the average discharge of 2014. Flood events were defined as starting and ending when discharge was more than 1.2-times the previous baseflow. Daily observed loads (OL) were calculated as products of the concentration and river discharge. The sums of discrete daily loads over various periods (flood events, months, seasons and annual) were used as references for evaluation of model performance.

2.4. LOADEST model calibration and evaluation

LOADEST assists researchers to develop a regression model to estimate constituent loads in rivers and streams. The model is formulated using seven parameters representing river discharge, time-trends, and seasonality (Eq. (1)) (Runkel et al., 2004).

$$\ln(L) = a_0 + a_1 \ln Q + a_2 \ln Q^2 + a_3 \sin(2\Pi dtime) + a_4 \cos(2\Pi dtime) + a_5 dtime + a_6 dtime^2 \quad (1)$$

where L is load; Q is stream flow or river discharge; dtime is decimal time; a_0 to a_6 are coefficients. The expressions lnQ and dtime are centered over the studied period to avoid multi-collinearity. For

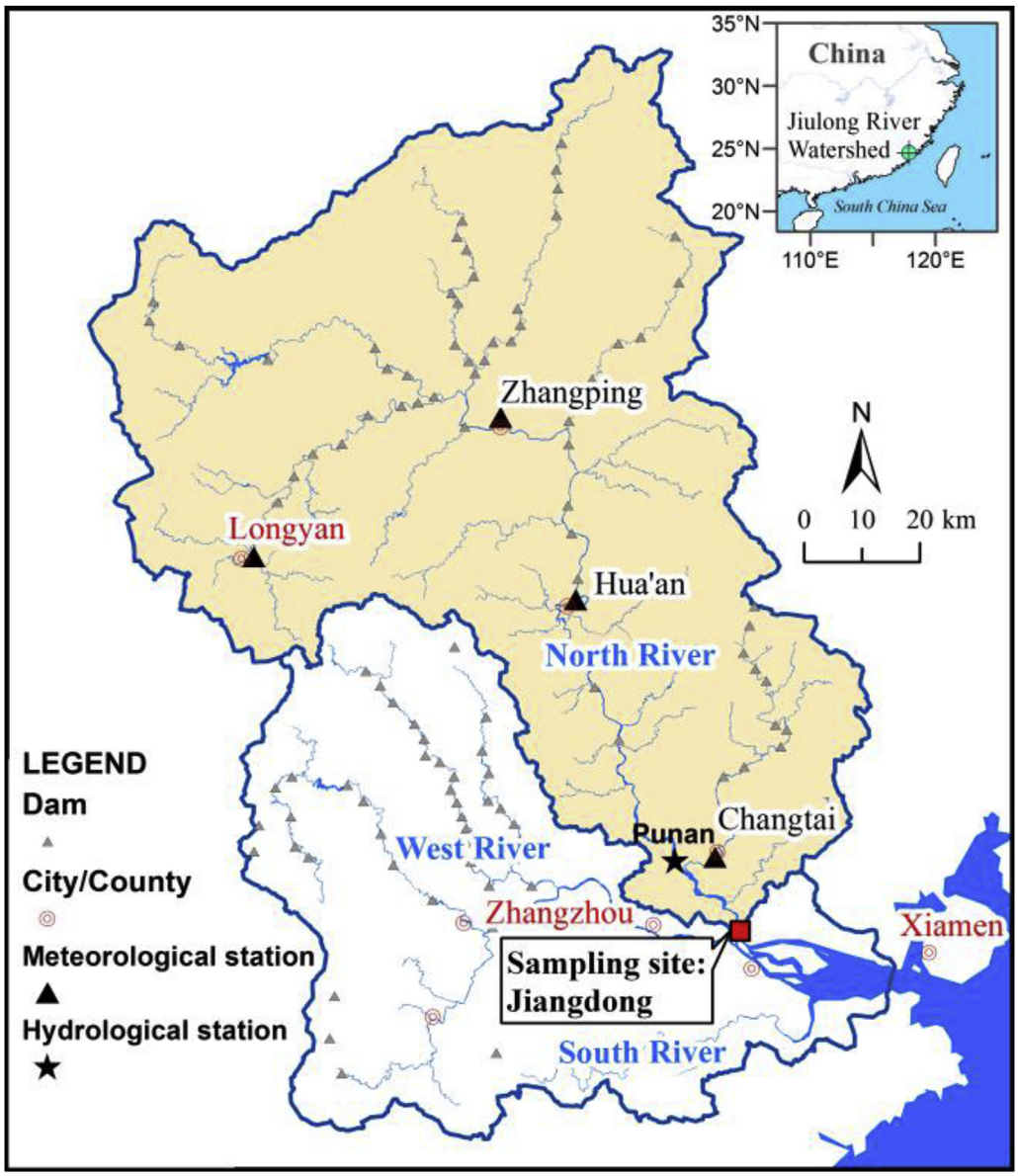

Fig. 1. Map of the Jiulong River watershed showing the study area, sampling site (square), river dam (grey triangle), the hydrological station Punan (star) and meteorological stations (black triangle). Jiangdong at the mouth of the North Jiulong River was selected as the sampling site for daily measurements of nitrogen concentrations in 2014.

instance, lnQ = ln(Q) - center of ln(Q) (Cohn et al., 1992). The LOADEST program provides predefined models comprising a minimum of the first two terms, with inclusion of additional terms. A "best" model can be automatically selected from the set of predefined models according to the lowest Akaike information criterion (AIC) (Akaike, 1981).

All daily data were grouped for different purposes of calibration. The "Year-round model" was developed directly using all daily concentrations and discharges in 2014. The "Piecewise model" was developed respectively for three periods (pre-wet season, wet season and post-wet season). We considered the period from May to September as the wet season according to the hydrology and nutrient characteristics of the studied watershed. We calibrated regression model coefficients based on AMLE (the adjusted maximum likelihood estimation) (Cohn, 1988). The AMLE method assumes a normal distribution of model residuals checked by a probability plot correlation coefficient (PPCC). A PPCC of 1.0 expresses a perfect normal probability of the calibration model residuals (Helsel and Hirsch, 2002). Sensitivity analysis of the model was carried out by assessing how each coefficient (1% increase or decrease) influences the estimated loads. Nash-Sutcliffe efficiency index (Nash and Sutcliffe, 1970) calculated by the LOADEST program and relative error (RE) (Eq. (2)) were used to compare model performance in estimating ammonium and nitrate loads.

$$RE(\%) = ([EL - OL]/OL) \times 100 \quad (2)$$

where EL is estimated load, and OL is observed load. RE equals 0 when the estimated load equals the observed load, and is < 0 when the regression model underestimates and >0 when the regression model overestimates.

To validate the model performance, we subsampled at three sampling frequencies (weekly, biweekly and monthly). In weekly samples, there are seven data sets starting from Monday through Sunday, respectively. In a similar way, biweekly and monthly

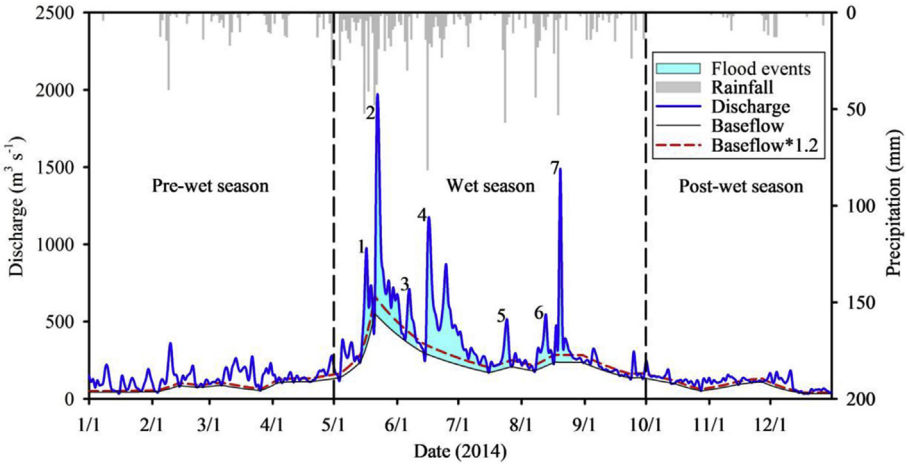

Fig. 2. Temporal variation of daily discharge of the North Jiulong River. Numbers (1–7) on the hydrograph indicate seven flood events in 2014.

sampling will produce 14 and 28 data sets (considering February has 28 days), respectively. These subsampled datasets were used as input to the "year-round" model. We then compared the estimated monthly N loads with measured loads.

Statistical analysis (ANOVA, regression, correlation) was performed using SPSS 17.0 at a significance level of $\alpha = 0.05$.

3. Results

3.1. Meteorological and hydrological conditions in 2014

The NJR watershed precipitation and river discharge showed obvious seasonal variations (Fig. 2). In 2014, total recorded rainfall was 1518 mm (long-term mean annual precipitation is 1564 mm), 75% of which occurred from May to September (wet season). Seven storms hit the basin in this year (the meteorological definition of a rain storm is daily rainfall greater than 50 mm). Daily discharge of NJR fluctuated from 34 to 1836 $m^3 s^{-1}$, averaging 235 $m^3 s^{-1}$, and thus close to the long-term mean annual discharge of 267 $m^3 s^{-1}$ (Punan). Cumulative runoff was 775 mm, accounting for 51% of annual rainfall (runoff coefficient = 0.51). For these reasons, 2014 was considered as a normal hydrologic year in this subtropical monsoon climate.

The rainfall events were accompanied by different hydrological responses in terms of duration and runoff. Seven flood events (hygrograph pulses) were identified and numbered sequentially (Fig. 2), all of which occurred in the wet season (May–September). The time delay between maximum precipitation and peak discharge was 1–5 days. Variations in soil moisture conditions prior to the discharge events were quantified by the Antecedent precipitation index (API; definition and values are given in Table 1). Flood 4 had the longest duration of 32 days due to persistent rainfall (Table 2), while floods 1, 3, 5 and 6 each lasted about one week. Flood 2 was the most extreme flood event with the highest peak discharge (1836 $m^3 s^{-1}$) and runoff coefficient (0.58).

3.2. River ammonium and nitrate concentrations and loads

Daily concentrations of ammonium and nitrate at the river mouth (Jiangdong) exhibited highly dynamic variations over the hydrographic cycle (Fig. 3). Nitrate varied from 1.42 to 5.04 mg N L^{-1} and ammonium from 0.11 to 2.35 mg N L^{-1}. Nitrate concentration was overall lower in the wet season than other seasons. Nitrate concentration was high in early 2014 in the pre-wet season and peaked at the end of March. Thereafter, it decreased gradually with a sharp decline during the first and second floods, before elevating again after July. In contrast, ammonium reached its peak in the middle of March, two weeks earlier than nitrate, followed by a slow decrease in the wet season before rising again at the end of the year. Plots of concentrations against discharge show clear seasonal pattern (Fig. 4). There was no significant correlation between concentration and discharge but the mean concentrations of nitrate and ammonium were significantly different across seasons (ANOVA, $P < 0.01$). Mean concentration of

Table 1
Meteorological and hydrological characteristics of flood events in 2014.

Flood events	Date	Duration	Peak rainfall	Average runoff	Peak discharge	Cumulative runoff	Runoff coefficient	API
		(d)	(mm h^{-1})	($m^3 s^{-1}$)	($m^3 s^{-1}$)	(mm)		(mm)
1	5/14–5/20	7	128.6	599.1	975.2	37.9	0.29	41.04 (III)
2	5/21–6/3	14	181.8	839.0	1836.0	106.0	0.58	76.90 (III)
3	6/5–6/11	7	62.7	496.5	710.6	31.4	0.50	32.96 (III)
4	6/15–7/16	32	248.6	459.6	1112.4	133.0	0.53	17.48 (II)
5	7/21–7/28	8	94.2	305.6	508.7	22.1	0.23	2.57 (I)
6	8/8-8/16	9	94.2	338.5	544.3	27.5	0.29	11.96 (I)
7	8/17–8/26	10	89.2	474.0	1490.4	42.8	0.48	30.65 (III)
Total		87				401.0		

Note: Mean rainfall was calculated using recorded hourly rainfall from four weather stations (Longyan, Zhangping, Hua'an and Changtai) in the North River. Peak delay is the time between the maximum rainfall in catchment and the peak water flow past stations Punan (PN) (Fig. 1). Cumulative runoff was calculated as total water mass divided by catchment area. Runoff coefficient was the ratio of cumulative runoff to rainfall. Antecedent precipitation index (API) = $\sum k^i P_i$, where P_i are precipitation 1, 2, …, i (i = 14) days prior to the event and k is a constant ($k = 0.85$). Three soil antecedent moisture conditions were classified according to API value. Condition I (dry): 0 ≤ API≤15 mm; Condition II (average): 15 ≤ API≤30 mm; Condition III (wet): API>30 mm. Adapted from Perrone and Madramootoo (1998).

Table 2
Comparison of the observed and estimated river nitrogen loads by the seasonal piecewise models.

Period	NH_4–N			NO_3–N		
	Observed load (10^5 kg)	Estimated load (10^5 kg)	Relative error (%)	Observed load (10^5 kg)	Estimated load (10^5 kg)	Relative error (%)
Flood 1	2.97	2.90	−2.5	9.64	8.53	−11.5
Flood 2	6.43	7.09	10.3	17.55	20.15	14.8
Flood 3	1.84	1.87	1.7	5.55	5.68	2.4
Flood 4	7.70	7.34	−4.7	25.91	24.62	−5.0
Flood 5	1.21	1.18	−2.1	4.31	4.63	7.3
Flood 6	1.69	1.70	0.2	6.04	6.04	0.0
Flood 7	2.64	2.87	8.6	10.24	9.27	−9.5
Pre-wet season	16.11	16.00	−0.7	49.52	49.54	0.1
Wet season	31.87	32.35	1.5	112.74	112.37	−0.3
Post-wet season	4.01	3.76	−6.2	28.32	28.32	0.0
Total (2014)	51.99	52.11	0.2	190.58	190.23	−0.2

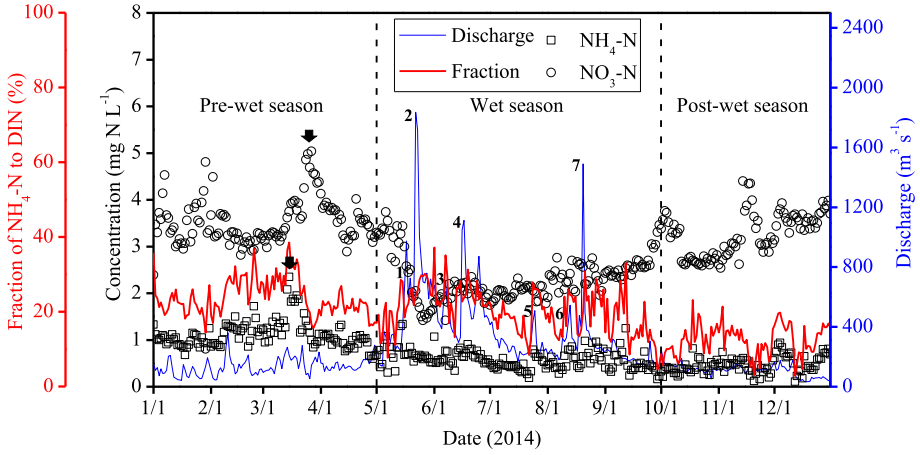

Fig. 3. Temporal variation of daily ammonium and nitrate concentration and the fraction of ammonium to DIN at the mouth (Jiangdong) of North Jiulong River in 2014. Arrows indicate nitrogen peaks in pre-wet season (March) caused by small rainfall events. Numbers (1–7) on the hydrography indicate seven flood events in 2014.

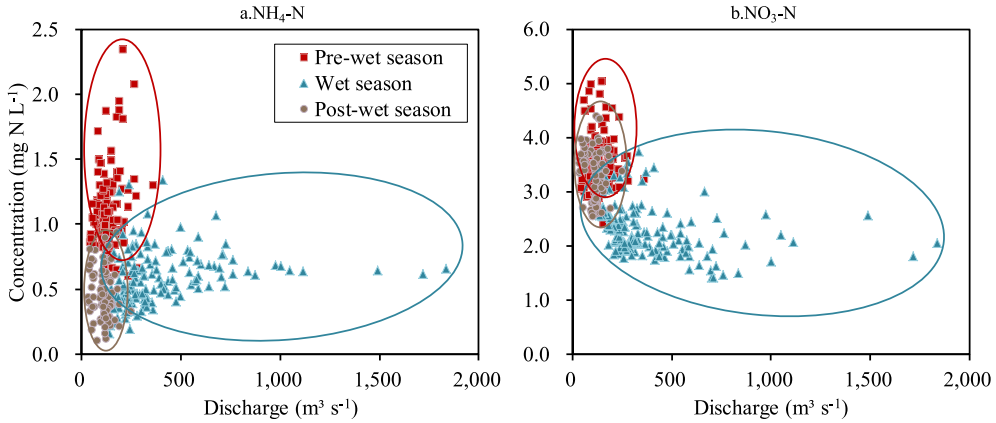

Fig. 4. Relationships between daily discharge and ammonium (a) and nitrate (b).

nitrate in pre-wet, wet, and post-wet seasons is 3.54, 2.31, 3.27 mg N L^{-1}, respectively; Mean concentration of ammonium is 1.12, 0.58, 0.47 mg N L^{-1}, respectively. For the seven flood events, the flow-weighted mean concentration in the rising limb of hydrograph was always greater than in the falling limb (ANOVA, $P < 0.01$). In addition, the maximum to minimum ratio (MMR) as an index of strength in storm induced N variation were calculated for each flood event, and this showed that ammonium MMR decreased with API (Fig. 5a) and nitrate MMR increased with mean discharge (Fig. 5b).

Overall, nitrate dominated DIN in river but varied with seasons (60%–97%). Ammonium accounted for an average of 17% of DIN a week prior to the first flood then increased to a maximum of 29%–37% during flood events. Most ammonium fraction peaked in the rising limb of the hydrograph (floods 1, 3, 5, 6). The highest ammonium fraction was 39% of DIN in March when its concentration peaked. High ammonium fractions were also found on the falling hydrograph for extreme flood 2 (37%) and flood 7 (31%).

Ammonium and nitrate loads in the wet season accounted for 61% and 59% of annual loads respectively in 2014. Seven flood

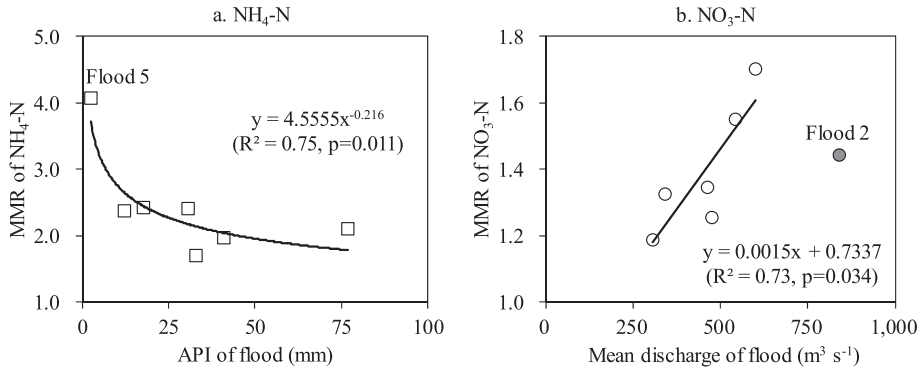

Fig. 5. Relationship between ammonium MMR (maximum to minimum ratio) and API (a) and between nitrate MMR and discharge of flood (b). The largest flood 2 was not included in the linear regression of nitrate against discharge.

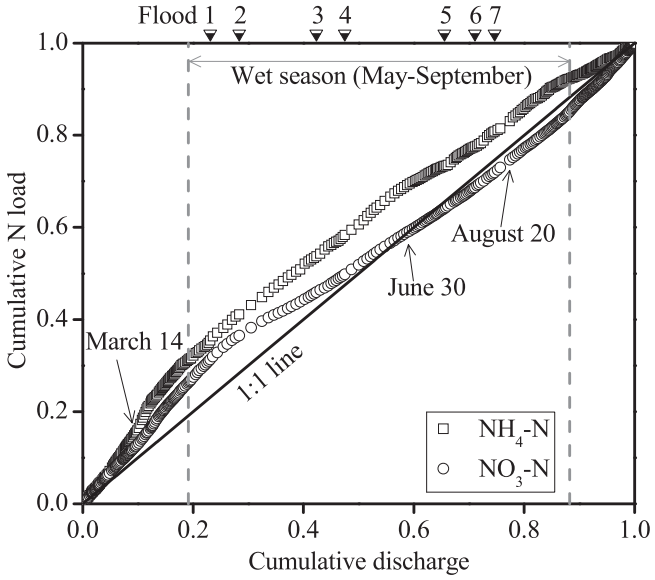

Fig. 6. Relationships between cumulative nitrogen loads and discharge in the North Jiulong River. The values on the line suggest nitrogen load and discharge are proportional, those above and below the 1:1 line expresses nutrient load mainly arrived towards the start, or end of the period, respectively. Arrows with dates show the turning points where load-discharge relationship changed. Numbers (1–7) on the top indicate the timing of seven flood events in 2014.

events in the wet season lasted 24% of the time and contributed 52% of the cumulative runoff, exporting 47% of ammonium and 42% of nitrate loads in 2014 (Table 2). Taking the "pollutogram" approach (Rossi et al., 2005; Stutter et al., 2008), relationships between cumulative N loads versus cumulative discharge showed that ammonium and nitrate had different timings of export (Fig. 6). The ammonium curve was always above the 1:1 line, suggesting that ammonium was mainly exported by discharge in the pre-wet season and wet season (with a turning point in mid-March when its concentration peaked). The nitrate curve was also above the 1:1 line but it went down in mid-May till passing below the 1:1 line in late June. The nitrate curve went up again in late August and onward toward the end of the year. The majority of nitrate exports occurred in the pre-wet and post-wet seasons.

3.3. Model performance of river ammonium and nitrate loads

A best model was selected based on the lowest AIC and then coefficients were calibrated using AMLE. For example, for the year-round model of NH_4–N, the lowest AIC was 0.702 (other predefined models had a higher AIC ranging from 0.822 to 1.511). Each PPCC of calibrated LOADEST models were close to 1, indicating a perfect normal probability of the model residuals. Sensitivity analysis of model coefficients suggested that a_0 in Eq. (1) was the most sensitive to both ammonium and nitrate load estimated by either the year-round models or the piecewise models (Table 3). The piecewise LOADEST model performed better than the year-round model in estimating monthly ammonium and nitrate loads (Table 3 and Fig. 7). The RE of ammonium load estimated by the year-round model was from −23.7% to 22%, while the RE of nitrate load estimation ranged from −11.5% to 12.5%. For the piecewise model, RE ranged from −8.7% to 7.8% for ammonium, and from −5.6% to 5.9% for nitrate. We focus on the piecewise model in the following discussion.

Flood event-based modeling results showed that the estimated ammonium loads had smaller deviations from observed values than nitrate during most flood events (Table 2). RE of ammonium ranged from −4.7% to 10.3%, while nitrate ranged from −11.5% to 14.8%. Nitrate and ammonium loads were underestimated in the first flood (flood 4 as well) of year 2014, but were overestimated in the subsequent floods 2–3, particularly for the extreme flood 2 (with largest RE). Ammonium concentration increased during the rising limb of the hydrograph in flood 1, while nitrate decreased before an increase in the falling limb in flood 2 (Fig. 8). In general, when N concentrations continually increase, the LOADEST model tends to underestimate N loads, and vice versa. Flood 6 had relatively small rainfall and discharge, and the best model performance. Other flood events produced good model results (absolute value of RE less than 10%) although they were somewhat overestimated or underestimated.

4. Discussion

4.1. Hydrological controls on river N export

River N can originate from both point and non-point sources in human perturbed watersheds (Mayorga et al., 2010). Excessive N input to and export from the North Jiulong River watershed was dominated by anthropogenic sources, mainly comprised of fertilizer runoff, sewage, and manure wastes (Yu et al., 2015). As a result of varying N loading across various land uses, river N concentrations and compositions show a large spatial variation (Chen et al., 2013). Ammonium was very high in the upstream area (Longyan), while nitrate increased and dominated DIN in the lower river (Chen et al., 2014). In March, in the pre-wet period when the first seasonal precipitations began, ammonium and nitrate increased

Table 3
The optimized LOADEST models and associated coefficients.

Nitrogen form	Calibration dataset by period	AIC	PPCC	NSE	Coefficients of selected LOADEST model						
					a0	a1	a2	a3	a4	a5	a6
NH_4–N	Year-round (2014)	0.702	0.985	0.846	9.37 (9.8%)	1.11 (-0.2%)	−0.04 (-0.02%)	−0.26 (0.0002%)	−0.22 (0.0001%)	−0.71 (0.0002%)	
	Pre-wet season	−0.539	0.995	0.826	−3.52 (-3.5%)	1.07 (0.1%)	0.04 (0.0%)	3.36 (0.02%)	12.97 (11.4%)	−19.09 (0.02%)	221.42 (2.0%)
	Wet-season	0.517	0.992	0.894	10.30 (10.9%)	1.33 (-0.3%)	−0.24 (-0.1%)	1.73 (0.01%)	−0.43 (-0.3%)	−9.09 (0.01%)	
	Post-wet season	0.195	0.990	0.705	7.79 (8.1%)	1.12 (0.3%)		−7.66 (0.5%)	0.20 (0.2%)	47.17 (-0.4%)	
NO_3–N	Year-round (2014)	−0.985	0.996	0.894	10.98 (11.6%)	0.90 (-0.1%)	−0.05 (-0.03%)	−0.16 (0.0001%)	−0.36 (0.0003%)	0.15 (0.00001%)	−1.66 (-0.1%)
	Pre-wet season	−1.386	0.987	0.933	23.77 (26.8%)	1.00 (0.1%)	0.02 (0.003%)	1.56 (0.003%)	−13.37 (-10.5%)	−8.54 (0.003%)	(-2.2%)
	Wet-season	−1.372	0.995	0.937	4.31 (4.4%)	0.99 (-0.2%)	−0.05 (-0.02%)	1.27 (0.003%)	6.88 (5.2%)	−6.45 (0.003%)	130.08 (1.9%)
	Post-wet season	−1.829	0.967	0.916	−28.09 (-24.5%)	1.01 (0.2%)	−0.05 (-0.01%)	4.84 (0.02%)	38.14 (41.0%)	−27.50 (0.02%)	728.92 (4.0%)

Note: AIC: Akaike information criterion; PPCC: probability plot correlation coefficient; NSE: Nash–Sutcliffe efficiency index.
Percentage values in parentheses below each coefficient indicate estimated loads change as their coefficients increase by 1%.

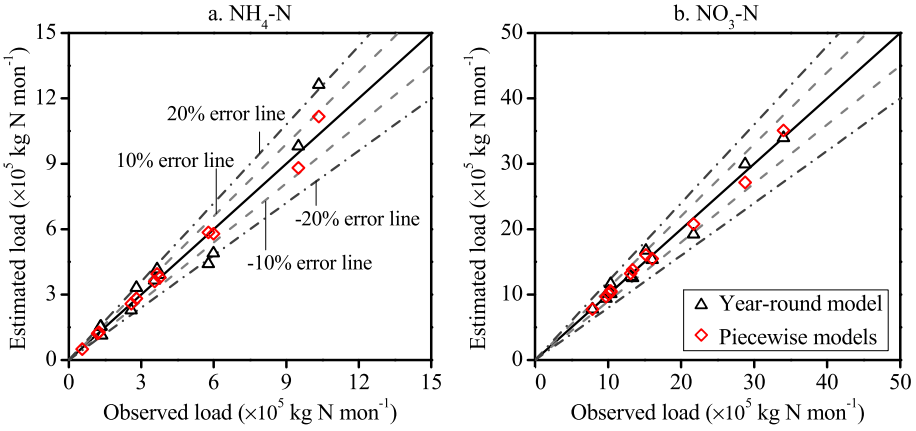

Fig. 7. Comparison of the observed and estimated monthly nitrogen loads by the seasonally piecewise models versus year-round model.

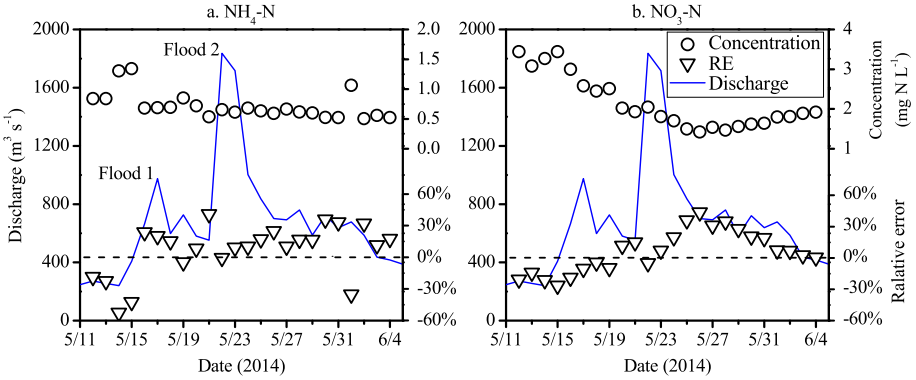

Fig. 8. Changes in river nitrogen concentrations corresponding to relative error (RE) of the estimated values over the hydrography of flood events 1 and 2.

significantly and ammonium reached its peak two weeks earlier than nitrate (Fig. 3). Increased ammonium loading also occurred upstream at this time (March), as observed at a dam reservoir in the middle NJR (Mo et al., 2016). These results imply that ammonium and nitrate have different sources supply and transport pathways to the river. Ammonium associated pollutants (e.g., fertilizer, human and animal wastes) can be stored at the land surface and in top soil layers, whereas nitrate accumulates in ground water and in the river channel during baseflow periods. According to previous studies, ammonium is often mainly transferred by surface runoff, while nitrate supply is dominated by within-channel mobilization and recharge of ground water (i.e. via baseflow) (Buda and DeWalle, 2009; Chen et al., 2012; Wagner et al., 2008). After dilution of its concentrations by strong discharge during the wet season, nitrate appears to have been steadily enriched again by nitrification in soils when rainfall reduced in the post-wet season. Ammonium

increased more slowly after the wet season. Both ammonium and nitrate are not significantly correlated with discharge in each season (Fig. 4). Nevertheless, ammonium was reduced in the post-wet season and the lowest nitrate concentrations were observed in high flow periods. River N was highly dynamic but generally was enriched in dry seasons and diluted in the wet season.

Storm induced N variation in the river channel depends on the balance of source supply (enrichment) and mixing with storm water (dilution). Flood events caused strong dilution of river N concentrations, especially in floods 1 and 2. Overall, the flow-weighted mean concentration (FWMC) in the rising limb of the hydrograph of the seven floods were always greater than in the falling limb of the hydrograph (data not shown). The ammonium MMR (maximum to minimum ratio in terms of concentration) decreased with API and the largest value occurred in flood 5 with the lowest API (Fig. 5a). A longer accumulation of ammonium could be washed downriver by storm runoff and resulted in a larger fluctuation in river ammonium concentration. We speculated that overland runoff carrying ammonium offset the dilution, as we did not find a correlation between MMR and discharge. In contrast, the nitrate MMR was not correlated with API but was positively correlated with mean flood discharge (Fig. 5b). This suggested that river nitrate originating from ground water had been strongly diluted by major storms. Current findings indicate that extreme storm induced discharges would be likely to cause large variation in river N fluxes to the estuary and coastal zone.

The river discharge regulated the majority of nitrate and ammonium exports from the river to estuary. A good correlation between river discharge and daily nitrate load ($r = 0.94$, $p < 0.01$) and ammonium load ($r = 0.90$, $p < 0.01$) implied strong hydrological controls on river N export. This is possibly a general characteristic of subtropical eastern continental margins, given that study of seven contiguous small watersheds on the Atlantic Coastal Plain also showed that N fluxes were higher with higher precipitation (Correll et al., 1999). However, watershed hydrology regulates river nitrate and ammonium in different ways. As a result of the differing sources and major transport paths (overland runoff for ammonium versus ground water recharge for nitrate), relatively more ammonium was exported in the pre-wet and wet season, while nitrate exports occurred more strongly in the pre-wet and post-wet season (Fig. 6). These results demonstrated the different effects of hydrological conditions on the timing and magnitude of nitrate and ammonium exports under the Asian monsoon climate.

Normalized by catchment area, the observed DIN flux from NJR in 2014 was 2534 kg N km^{-2} yr^{-1}, which was greater than the 2005–2010 level (average 2107 kg N km^{-2} yr^{-1}) (Yu et al., 2015), and more than two times larger than the DIN fluxes from Changjiang (Yangtze) River (895 kg N km^{-2} yr^{-1} in 2003, one of the world's largest rivers) (Yan et al., 2010). Maximum monthly nitrate flux in 2014 was 355 kg N km^{-2}, nearly 6 times more than the nitrate flux from the Mississippi River (51 kg N km^{-2} in 2013) (Pellerin et al., 2014). Thus, the JR is very much a major source of nutrients to coastal waters, and our results have important implications for coastal aquatic ecology. Major storms and floods contributed large N exports (47% of annual ammonium load and 42% of annual nitrate load) in a short period (24% of the year) although their concentrations became lower (water quality improved). Notably, algae bloom events in the Jiulong River estuary and Xiamen Bay are usually observed 1–2 weeks after summer storms. Pulse input of large inorganic N with relatively abundant ammonium N (its fraction to DIN elevated from 17% before flood to 29–37% following floods) might have stimulated algal blooms. It has been demonstrated that many algae and dinoflagellates preferentially utilize ammonium rather than nitrate as N source (Dortch, 1990; Lomas and Glibert, 1999), and peaks of chlorophyll-a in the Chesapeake Bay water generally follow the peaks of ammonium input caused by rainfalls (Glibert et al., 2008). As shown in Fig. 3, the highest ammonium concentration and abundance (39% of DIN) caused by "first flush" of small rainfall events in March also present a high risk of spring algal blooms. Such an effect is defined as when peak concentration precedes peak discharge, and is often observed in human perturbed watersheds (Yoon and Stein, 2008). Further discussion of the hydrological linkages among river nutrient supply and coastal ecosystem responses is beyond the scope of this study and requires further research.

4.2. Processes affecting modeling of N loads and improvement

The year-round LOADEST model did not perform as well as the seasonally piecewise model in estimating monthly river N loads (Table 3), largely due to distinct relationships between concentration and discharge (Fig. 4). As a result of the relatively similar hydrological conditions for each modeling period (pre-wet, wet, and post-wet seasons), the piecewise model achieved better results (RE = 5–8%) than the year-round model (RE = 12–24%) (Fig. 7). Therefore, we recommend using the piecewise model to estimate river N loads in this area.

We found that extreme hydrological conditions (pulses of storm flow) produced greater deviations of estimated loads from observed values. When river N concentrations continued to increase during flooding periods, the LOADEST model (piecewise) tended to underestimate N load, and vice versa (Fig. 8). Model construction suggests that the river N load is a function of discharge and time. On the occasion of dramatic change in storm waters over short periods (i.e., during major storms and floods), watershed N can be flushed into waterways and exhibit either enrichment or dilution in river depending on N forms and antecedent soil conditions. After a long period of accumulation, river ammonium showed an obvious "first flush" effect as discharge rose following the first major storm of the year (e.g., in flood 1), followed by a dilution in the falling hydrograph. In this case, the piecewise LOADEST model for the wet season underestimated ammonium loads on the rising limb of the hydrograph and overestimated it on the falling hydrograph (Fig. 8a). Unlike ammonium, river nitrate was firstly diluted on the rising limb of the hydrograph and was only enriched by a delayed recharge of nitrate-rich ground water on the falling hydrograph (e.g., in flood events 1 and 2) (Fig. 8b). Therefore, the LOADEST model tended to overestimate nitrate load on the rising and underestimate on the falling hydrograph. Nevertheless, the model still works well over the whole flooding period as estimation biases offset each other between the rising and falling hydrographic periods.

The behaviors of LOADEST models differ not only by nutrient forms but also by proportion of storm samples and characteristics of watersheds (Chen et al., 2017; Park and Engel, 2015; Toor et al., 2008). Park and Engel (2014) stated that more frequent sampling did not necessarily lead to more accurate and precise annual pollutant load estimates. But at the monthly scale, the monthly nitrate loads based on sampling at biweekly to bimonthly intervals could be underestimated by up to 21% (Pellerin et al., 2014). In this study, the model behaviors with three sampling frequencies (weekly, biweekly, and monthly) were tested by adjusting the input dataset. This showed that RE of estimated ammonium and nitrate increase as the sampling frequency reduces (Table 4). Weekly and biweekly sampling would produce a sound estimation of monthly ($-0.3 \pm 8\%$) and annual nitrate loads ($-1 \pm 3\%$) but monthly sampling had a fairly large RE (Table 4). Current results indicate that ammonium is more dynamic than nitrate and requires a more intensive sampling in order to obtain a robust estimation of riverine loads.

Table 4
Relative error (RE) of estimated river nitrogen loads using the LOADEST model based on subsampled datasets at various sampling frequencies.

Nitrogen form	Estimates	RE by sampling frequency (%)		
		Weekly	Biweekly	Monthly
NH_4–N	Monthly load	3 ± 18	2 ± 22	6 ± 48
	Annual load	3 ± 4	3 ± 7	7 ± 29
NO_3–N	Monthly load	−0.3 ± 8	−0.3 ± 8	1 ± 16
	Annual load	−1±3	−1±3	0.3 ± 9

Note: Data presented as mean ± SD.

In an agricultural area like the Jiulong River watershed, non-point source dominates N loading and hydrology (discharge) controls the majority of river N exports to coast. However, climate change is likely to increase the occurrence and intensity of flood or drought (Domroes and Schaefer, 2008; Knutson et al., 2010; Planton et al., 2008). Extreme weather events and human activities (agricultural development, urbanization, dam construction, transboundary water transfer, etc.) will substantially alter watershed hydrological processes and further impact nutrient cycling and delivery to the river-estuary-coast continuum. Although the seasonally piecewise LOADEST model provides favorable outputs, more efforts are still required to advance our understanding and prediction of nutrient dynamics and discharges, including the following. (1) Long-term monitoring to examine nutrient biogeochemical cycling and export in relation to changing hydrology over years and decades. (2) Enhanced temporal resolution of measurements (hourly or sub-daily) to reduce uncertainties of observation, and capture rapid event dynamics, particularly for large floods. In this regard, our previous work suggests that river nutrient concentrations observed at an interval of 2 h captured a broader fluctuation in extreme storms (Chen et al., 2012, 2015). (3) Optimize the model structure including some more potential parameters (e.g., API, peak Q). In the context of increased extreme weather events under climate change, even if the N input to the watershed is constant, we argue that the LOADEST model is unlikely make a reasonable estimation on nutrient loads. Strauch et al. (2018) also suggest that LOADEST tended to underestimate sediment yield as it failed to capture the high variability in tropical streamflow. Therefore, integrating hydrologic extrema into modeling work to improve the relationship between N concentration and discharges deserves further study.

5. Conclusions

There is a strong seasonal variation in watershed precipitation and river discharge under the Asian monsoon climate of southeast China. Hydrological controls on the N export from an agricultural watershed (NJR) were examined based on daily measurements at the river mouth in a normal hydrologic year (2014). Contrasting temporal patterns and load-discharge relationships between ammonium and nitrate were observed, likely ascribed to their different sources and transport pathways to the river continuum. It appeared that ammonium was mainly transferred by surface runoff, but nitrate supply was dominated by within-channel mobilization and recharge of ground water. Both ammonium and nitrate concentrations increased significantly in March and ammonium reached its peak two weeks earlier than nitrate. Both ammonium and nitrate were diluted in the wet season and enriched in the dry season. Overall, hydrological processes regulated the majority of ammonium and nitrate fluxes from river to estuary, as suggested by good correlation between daily discharge and N load ($r > 0.90$). However, the “pollutogram” showing cumulative N loads versus river discharge indicated that relatively more ammonium was exported in the pre-wet and wet seasons, while nitrate exports occurred in both pre-wet and post-wet seasons. Seven flood events occurred in 2014 only lasted 24% of the year but contributed 52% accumulative runoff, exporting 47% of ammonium and 42% of nitrate loads. The differences in the timing and magnitude of N export between ammonium and nitrate across the seasons, and in responses to pulsed inputs of freshwater and inorganic N with relatively abundant ammonium in major floods, suggests that changing hydrology in our changing climate is likely to lead to significant changes in environmental conditions and ecological states in rivers, estuaries, and the coastal zone in this region.

The seasonal characteristic of the subtropical monsoon climate and watershed hydrology determined that the piecewise LOADEST model (for pre-wet, wet, and post-wet seasons) (5–8% error) performed better than the year-round model (12–24% error) in estimating monthly river N loads. Accordingly, we recommend using the piecewise model to estimate river N loads in subtropical regions. Although the model tended to overestimate river nitrate load on the rising hydrograph and underestimate on the falling hydrograph, while overestimating ammonium load on the falling hydrograph and underestimating on the rising hydrograph, it still performed well over the whole hydrograph as biases during most floods were less than 10%. However, extreme floods might produce greater deviations in modeling river N loads than is expected from the present model. Advancing our capability of nutrient estimation using the seasonally piecewise LOADEST model can be achieved by long-term monitoring and high-frequency measurements (hourly or sub-daily), and optimizing the model structure addressing hydrological extrema under global change.

Acknowledgments

This research was supported by the National Natural Science Foundation of China (No. 41376082; 41676098), the National Key Research and Development Program of China (2016YFC0502901), and the Project of Xiamen Southern Ocean Center (14GST68NF32). We thank Ting Lu and all peoples who assisted in sampling and lab analysis. Special thanks are given to Hydrological Station for providing hydrological data. We thank MEL Visiting Scholar Tom Trull for his useful comments on this manuscript.

References

Adame, M.F., Fry, B., Bunn, S.E., 2016. Water isotope characteristics of a flood: brisbane River, Australia. Hydrol. Process. 30, 2033–2041.
Akaike, H., 1981. Likelihood of a model and information criteria. J. Econom. 16, 3–14.
American Public Health Association, A.P.H.A, 2005. Standard Methods for the Examination of Water and Wastewater, 21th ed. APHA, Washington, DC, USA, pp. 9–72.
Arnold, J.G., Srinivasan, R., Muttiah, R.S., Williams, J.R., 1998. Large area hydrologic modeling and assessment Part I: model development. J. Am. Water Resour. Assoc. 34, 73–89.
Billen, G., Garnier, J., 2007. River basin nutrient delivery to the coastal sea: assessing its potential to sustain new production of non-siliceous algae. Mar. Chem. 106, 148–160.
Buda, A.R., DeWalle, D.R., 2009. Dynamics of stream nitrate sources and flow pathways during stormflows on urban, forest and agricultural watersheds in central Pennsylvania, USA. Hydrol. Process. 23, 3292–3305.
Chen, L., Sun, C., Wang, G., Xie, H., Shen, Z., 2017. Event-based nonpoint source pollution prediction in a scarce data catchment. J. Hydrol. 552, 13–27.
Chen, N., Peng, B., Hong, H., Turyaheebwa, N., Cui, S., Mo, X., 2013. Nutrient enrichment and N:P ratio decline in a coastal bay-river system in southeast China: the need for a dual nutrient (N and P) management strategy. Ocean Coast Manag. 81, 7–13.
Chen, N., Wu, J., Chen, Z., Lu, T., Wang, L., 2014. Spatial-temporal variation of dissolved N_2 and denitrification in an agricultural river network, southeast China. Agric. Ecosyst. Environ. 189, 1–10.
Chen, N., Wu, J., Hong, H., 2012. Effect of storm events on riverine nitrogen dynamics in a subtropical watershed, southeastern China. Sci. Total Environ. 431, 357–365.

Chen, N., Wu, Y., Chen, Z., Hong, H., 2015. Phosphorus export during storm events from a human perturbed watershed, southeast China: implications for coastal ecology. Estuar. Coast. Shelf Sci. 166, 178–188.
Cohn, T.A., 1988. Adjusted Maximum Likelihood Estimation of the Moments of Lognormal Populations from Type I Censored Samples. U.S. Geological Survey.
Cohn, T.A., Caulder, D.L., Gilroy, E.J., Zynjuk, L.D., Summers, R.M., 1992. The validity of a simple statistical model for estimating fluvial constituent loads: an Empirical study involving nutrient loads entering Chesapeake Bay. Water Resour. Res. 28, 2353–2363.
Cornelis, J.T., Delvaux, B., Georg, R.B., Lucas, Y., Ranger, J., Opfergelt, S., 2011. Tracing the origin of dissolved silicon transferred from various soil-plant systems towards rivers: a review. Biogeosciences 8, 89–112.
Correll, D.L., Jordan, T.E., Weller, D.E., 1999. Effects of precipitation and air temperature on nitrogen discharges from Rhode river watersheds. Water, Air, Soil Pollut. 115, 547–575.
Corriveau, J., Chambers, P.A., Culp, J.M., 2013. Seasonal variation in nutrient export along streams in the Northern Great Plains. Water, Air, Soil Pollut. 224.
Davidson, K., Gowen, R.J., Harrison, P.J., Fleming, L.E., Hoagland, P., Moschonas, G., 2014. Anthropogenic nutrients and harmful algae in coastal waters. J. Environ. Manag. 146, 206–216.
De Carlo, E.H., Hoover, D.J., Young, C.W., Hoover, R.S., Mackenzie, F.T., 2007. Impact of storm runoff from tropical watersheds on coastal water quality and productivity. Appl. Geochem. 22, 1777–1797.
Domingues, R.B., Barbosa, A.B., Sommer, U., Galvão, H.M., 2011. Ammonium, nitrate and phytoplankton interactions in a freshwater tidal estuarine zone: potential effects of cultural eutrophication. Aquat. Sci. 73, 331–343.
Domroes, M., Schaefer, D., 2008. Recent climate change affecting rainstorm occurrences: a case study in East China. Clim. Past 4, 303–309.
Dortch, Q., 1990. The interaction between ammonium and nitrate uptake in phytoplankton. Mar. Ecol. Prog. 61, 183–201.
Duan, S., Powell, R.T., Bianchi, T.S., 2014. High frequency measurement of nitrate concentration in the Lower Mississippi River, USA. J. Hydrol. 519, 376–386.
Dugdale, R.C., Wilkerson, F.P., Hogue, V.E., Marchi, A., 2007. The role of ammonium and nitrate in spring bloom development in San Francisco Bay. Estuar. Coast Shelf Sci. 73, 17–29.
Glibert, P.M., Kelly, V., Alexander, J., Codispoti, L.A., Boicourt, W.C., Trice, T.M., Michael, B., 2008. In situ nutrient monitoring: a tool for capturing nutrient variability and the antecedent conditions that support algal blooms. Harmful Algae 8, 175–181.
Helsel, D.R., Hirsch, R.M., 2002. Statistical methods in water resources: U.S. Department of the Interior. In: Groat, C.G. (Ed.), Techniques of Water-Resources Investigations of the United States Geological Survey. United States Geological Survey.
Howarth, R.W., 2008. Coastal nitrogen pollution: a review of sources and trends globally and regionally. Harmful Algae 8, 14–20.
Hunter, H.M., Walton, R.S., 2008. Land-use effects on fluxes of suspended sediment, nitrogen and phosphorus from a river catchment of the Great Barrier Reef, Australia. J. Hydrol. 356, 131–146.
Johnson, M.S., Woodbury, P.B., Pell, A.N., Lehmann, J., 2007. Land-use change and stream water fluxes: decadal dynamics in watershed nitrate exports. Ecosystems 10, 1182–1196.
Knutson, T.R., McBride, J.L., Chan, J., Emanuel, K., Holland, G., Landsea, C., Held, I., Kossin, J.P., Srivastava, A.K., Sugi, M., 2010. Tropical cyclones and climate change. Nat. Geosci. 3, 157–163.
Li, Y., Cao, W., Su, C., Hong, H., 2011. Nutrient sources and composition of recent algal blooms and eutrophication in the northern Jiulong River, Southeast China. Mar. Pollut. Bull. 63, 249–254.
Lomas, M.W., Glibert, P.M., 1999. Interactions between NH_4+ and NO_3- uptake and assimilation: comparison of diatoms and dinoflagellates at several growth temperatures. Mar. Biol. 133, 541–551.
Mast, M.A., 2013. Evaluation of stream chemistry trends in US Geological Survey reference watersheds, 1970–2010. Environ. Monit. Assess. 185, 9343–9359.
Mayorga, E., Seitzinger, S.P., Harrison, J.A., Dumont, E., Beusen, A.H.W., Bouwman, A.F., Fekete, B.M., Kroeze, C., Van Drecht, G., 2010. Global Nutrient export from WaterSheds 2 (NEWS 2): model development and implementation. Environ. Model. Software 25, 837–853.
Mo, Q.L., Chen, N.W., Zhou, X.P., Chen, J.X., Duan, S.W., 2016. Ammonium and phosphate enrichment across the dry-wet transition and their ecological relevance in a subtropical reservoir, China. Environ. Sci. Process. Impact 18, 882–894.
Nash, J.E., Sutcliffe, J.V., 1970. River flow forecasting through conceptual models part I — a discussion of principles. J. Hydrol. 10, 282–290.
Paerl, H.W., 2006. Assessing and managing nutrient-enhanced eutrophication in estuarine and coastal waters: interactive effects of human and climatic perturbations. Ecol. Eng. 26, 40–54.
Paerl, H.W., Hall, N.S., Calandrino, E.S., 2011. Controlling harmful cyanobacterial blooms in a world experiencing anthropogenic and climatic-induced change. Sci. Total Environ. 409, 1739–1745.
Park, Y.S., Engel, B.A., 2014. Use of pollutant load regression models with various sampling frequencies for annual load estimation. Water 6, 1685–1697.
Park, Y.S., Engel, B.A., 2015. Analysis for regression model behavior by sampling strategy for annual pollutant load estimation. J. Environ. Qual. 44, 1843–1851.
Peñuelas, J., Poulter, B., Sardans, J., Ciais, P., Van, D.V.M., Bopp, L., Boucher, O., Godderis, Y., Hinsinger, P., Llusia, J., 2013. Human-induced nitrogen-phosphorus imbalances alter natural and managed ecosystems across the globe. Nat. Commun. 4, 2934.
Pellerin, B.A., Bergamaschi, B.A., Gilliom, R.J., Crawford, C.G., Saraceno, J., Frederick, C.P., Downing, B.D., Murphy, J.C., 2014. Mississippi river nitrate loads from high frequency sensor measurements and regression-based load estimation. Environ. Sci. Technol. 48, 12612–12619.
Perrone, J., Madramootoo, C.A., 1998. Improved curve numberselection for runoff prediction. Can. J. Civil Eng. 25, 728–734.
Planton, S., Déqué, M., Chauvin, F., Terray, L., 2008. Expected impacts of climate change on extreme climate events. Compt. Rendus Geosci. 340, 564–574.
Reed, M.L., Pinckney, J.L., Keppler, C.J., Brock, L.M., Hogan, S.B., Greenfield, D.I., 2016. The influence of nitrogen and phosphorus on phytoplankton growth and assemblage composition in four coastal, southeastern USA systems. Estuar. Coast. Shelf Sci. 177, 71–82.
Rossi, L., Krejci, V., Rauch, W., Kreikenbaum, S., Fankhauser, R., Gujer, W., 2005. Stochastic modeling of total suspended solids (TSS) in urban areas during rain events. Water Res. 39, 4188–4196.
Runkel, R., Crawford, C., Cohn, T., 2004. Load Estimator (LOADEST): A FORTRAN Program for Estimating Constituent Loads in Streams and Rivers. U.S. Department of the Interior; U.S. Geological Survey.
Sigleo, A.C., Frick, W.E., 2007. Seasonal variations in river discharge and nutrient export to a Northeastern Pacific estuary. Estuar. Coast. Shelf Sci. 73, 368–378.
Statham, P.J., 2012. Nutrients in estuaries – an overview and the potential impacts of climate change. Sci. Total Environ. 434, 213–227.
Strauch, A.M., MacKenzie, R.A., Giardina, C.P., Bruland, G.L., 2018. Influence of declining mean annual rainfall on the behavior and yield of sediment and particulate organic carbon from tropical watersheds. Geomorphology 306, 28–39.
Strokal, M., Kroeze, C., Wang, M., Bai, Z., Ma, L., 2016. The MARINA model (model to assess river inputs of Nutrients to seas): model description and results for China. Sci. Total Environ. 562, 869–888.
Strokal, M., Yang, H., Zhang, Y., Kroeze, C., Li, L., Luan, S., Wang, H., Yang, S., Zhang, Y., 2014. Increasing eutrophication in the coastal seas of China from 1970 to 2050. Mar. Pollut. Bull. 85, 123–140.
Stutter, M.I., Langan, S.J., Cooper, R.J., 2008. Spatial contributions of diffuse inputs and within-channel processes to the form of stream water phosphorus over storm events. J. Hydrol. 350, 203–214.
Tamminen, T., 1995. Nitrate and ammonium depletion rates and preferences during a Baltic spring bloom. Mar. Ecol. Prog. Ser. 120, 123–133.
Toor, G.S., Harmel, R.D., Haggard, B.E., Schmidt, G., 2008. Evaluation of regression methodology with low-frequency water quality sampling to estimate constituent loads for ephemeral watersheds in Texas. Journal of Environment Quality 37, 1847.
Turner, R.E., Rabalais, N.N., 1994. Coastal eutrophication near the Mississippi river delta. Nature 368, 619–621.
Wagner, L.E., Vidon, P., Tedesco, L.P., Gray, M., 2008. Stream nitrate and DOC dynamics during three spring storms across land uses in glaciated landscapes of the Midwest. J. Hydrol. 362, 177–190.
Wang, G., Fang, Q., Zhang, L., Chen, W., Chen, Z., Hong, H., 2010. Valuing the effects of hydropower development on watershed ecosystem services: case studies in the Jiulong River Watershed, Fujian Province, China. Estuar. Coast. Shelf Sci. 86, 363–368.
Wang, P.F., Martin, J., Morrison, G., 1999. Water quality and eutrophication in Tampa bay, Florida. Estuar. Coast. Shelf Sci. 49, 1–20.
Yan, W., Mayorga, E., Li, X., Seitzinger, S.P., Bouwman, A.F., 2010. Increasing anthropogenic nitrogen inputs and riverine DIN exports from the Changjiang River basin under changing human pressures. Global Biogeochem. Cycles 24, GB0A06.
Yan, X., Zhai, W., Hong, H., Li, Y., Guo, W., Huang, X., 2012. Distribution, fluxes and decadal changes of nutrients in the Jiulong River estuary, Southwest Taiwan strait. Chin. Sci. Bull. 57, 2307–2318.
Yoon, V.K., Stein, E.D., 2008. Natural catchments as sources of background levels of storm-water metals, nutrients, and solids. J. Environ. Eng. 134, 967–973.
Yu, D., Yan, W., Chen, N., Peng, B., Hong, H., Zhuo, G., 2015. Modeling increased riverine nitrogen export: source tracking and integrated watershed-coast management. Mar. Pollut. Bull. 101, 642–652.
Zhang, J.Z., Kelble, C.R., Fischer, C.J., Moore, L., 2009. Hurricane Katrina induced nutrient runoff from an agricultural area to coastal waters in Biscayne Bay, Florida. Estuar. Coast. Shelf Sci. 84, 209–218.